RAA 2017 Vol. **17** No. **11**, 118 (18pp) doi: 10.1088/1674–4527/17/11/118

http://www.raa-journal.org *http://iopscience.iop.org/raa*

***R**esearch in*
***A**stronomy and*
***A**strophysics*

Correlation among extinction efficiency and other parameters in an aggregate dust model

Tanuj Kumar Dhar and Himadri Sekhar Das

Department of Physics, Assam University, Silchar 788011, India; *hsdas13@gmail.com*

Received 2017 February 28; accepted 2017 August 25

Abstract We study the extinction properties of highly porous Ballistic Cluster-Cluster Aggregate dust aggregates in a wide range of complex refractive indices ($1.4 \leq n \leq 2.0$, $0.001 \leq k \leq 1.0$) and wavelengths ($0.11\,\mu\mathrm{m} \leq \lambda \leq 3.4\,\mu\mathrm{m}$). An attempt has been made for the first time to investigate the correlation among extinction efficiency (Q_{ext}), composition of dust aggregates (n, k), wavelength of radiation (λ) and size parameter of the monomers (x). If k is fixed at any value between 0.001 and 1.0, Q_{ext} increases with increase of n from 1.4 to 2.0. Q_{ext} and n are correlated via *linear* regression when the cluster size is small, whereas the correlation is *quadratic* at moderate and higher sizes of the cluster. This feature is observed at all wavelengths (ultraviolet to optical to infrared). We also find that the variation of Q_{ext} with n is very small when λ is high. When n is fixed at any value between 1.4 and 2.0, it is observed that Q_{ext} and k are correlated via a polynomial regression equation (of degree 1, 2, 3 or 4), where the degree of the equation depends on the cluster size, n and λ. The correlation is linear for small size and quadratic/cubic/quartic for moderate and higher sizes. We have also found that Q_{ext} and x are correlated via a polynomial regression (of degree 3, 4 or 5) for all values of n. The degree of regression is found to be n and k-dependent. The set of relations obtained from our work can be used to model interstellar extinction for dust aggregates in a wide range of wavelengths and complex refractive indices.

Key words: light scattering — ISM: dust, extinction

1 INTRODUCTION

The studies of cometary and interplanetary dust indicate that cosmic dust grains are likely to be fluffy, porous and composites of many small grains fused together, due to dust-gas interactions, grain-grain collisions and various other processes (Krueger & Kissel 1989; Greenberg & Hage 1990; Wolff et al. 1994). Porous, composite aggregates are often modeled as clusters of small spheres (known as "monomers"), agglomerated under various aggregation rules. Here grain aggregates are assumed to be fluffy sub-structured collections of very small particles loosely attached to one another. Each particle is assumed to consist of a single material, such as silicates or carbon, as formed in the various separate sources of cosmic dust. Extinction generally takes place whenever electromagnetic radiation propagates through a medium containing small particles. The spectral dependence of extinction, or extinction curve, is a function of the structure, composition and size distribution of the particles. The study of interstellar extinction provides us with useful information for understanding the properties of the dust.

It is now well accepted from observation and laboratory analysis of interplanetary dust particles that cosmic dust grains are *fluffy aggregates* or *porous* with irregular shapes (Brownlee 1985; Mathis & Whiffen 1989; Greenberg & Hage 1990). Using the Discrete Dipole Approximation (DDA) technique, several investigators studied the extinction properties of the composite grains (Wolff et al. 1994, 1998; Voshchinnikov et al. 2006; Vaidya & Gupta 1999; Vaidya et al. 2007; Vaidya & Gupta 2009). Iatì et al. (2004) studied opti-

cal properties of composite grains as grain aggregates of amorphous carbon and astronomical silicates, using the superposition transition matrix approach. Recently, Mazarbhuiya & Das (2017) studied the light scattering properties of aggregate particles in a wide range of complex refractive indices and wavelengths to investigate the correlation among different parameters, e.g., the positive polarization maximum, the amplitude of negative polarization, geometric albedo, refractive indices and wavelength. The simulations were performed using the Superposition T-matrix code with Ballistic Cluster-Cluster Aggregate (BCCA) particles of 128 monomers and Ballistic Aggregate particles of 512 monomers.

The extinction efficiency of dust aggregates depends on aggregate size, composition and wavelength of incident radiation. The dependence of complex refractive index (n, k) on $Q_{\rm ext}$ was studied by many groups in the past for spherical and irregular particles using different scattering theories (Mie theory, DDA approach, T-matrix theory, etc.). However, no correlation equations were reported earlier by any group. In this paper, we study the extinction properties of randomly oriented porous dust aggregates with a wide range of complex refractive indices and wavelengths of incident radiation. An attempt has been made for the first time to investigate the correlation among extinction efficiency ($Q_{\rm ext}$), complex refractive indices ($m = n + ik$), wavelength (λ) and the size parameter of a monomer (x).

2 NUMERICAL COMPUTATIONS

We have constructed the aggregates using the ballistic aggregation procedure (Meakin 1983, 1984) by applying two different models of cluster growth; first via single-particle aggregation and then through cluster-cluster aggregation. These aggregates were built by randomly hitting and sticking particles together. The first one is called Ballistic Particle-Cluster Aggregate (BPCA) when the method allows only single particles to join the cluster of particles. If the method allows clusters of particles to stick together, the aggregate is called a BCCA. Actually, BPCA clusters are more compact than BCCA clusters (Mukai et al. 1992). The porosity of BPCA and BCCA particles of 128 monomers has the values 0.90 and 0.94, respectively. The fractal dimensions of BPCA and BCCA particles are given by $D \approx 3$ and ≈ 2, respectively (Meakin 1984). A systematic explanation with the dust aggregate model is already discussed in our previous work (Das et al. 2008). It can be noted that the structures of these aggregates are similar to those of Interplanetary Dust Particles collected in the stratosphere of Earth (Brownlee 1985). It is also well understood from laboratory diagnosis that particle coagulation in the solar nebula grows under the BCCA process (Wurm & Blum 1998).

The general extinction A_λ is given by (Spitzer 1978)

$$A_\lambda = -2.5 \log \left[\frac{F(\lambda)}{F_0(\lambda)} \right] = 1.086\, N_{\rm d}\, Q_{\rm ext}\, \sigma_{\rm d}, \quad (1)$$

where $F(\lambda)$ and $F_0(\lambda)$ are the observed and expected fluxes, $N_{\rm d}$ is the dust column density, $Q_{\rm ext}$ is the extinction efficiency factor determined from the Superposition T-matrix code and $\sigma_{\rm d}$ is the geometrical cross-section of a single particle.

The interstellar extinction curve (i.e., the variation of extinction with wavelength) is usually expressed by the ratio $A_\lambda/E(B-V)$ versus 1/λ. The extinction curve covers the wavelength range 0.11 to 3.4 μm. The entire range consists of ultraviolet (UV), visible and infrared (IR) regions. The IR range corresponds to near IR, i.e. 0.750 to 2.5 μm, the visible range (0.38 to 0.76 μm) and the UV range (with the last part of violet in the visible spectrum to 0.11 μm).

The radius of an aggregate particle can be described by the radius of a sphere of equal volume given by $a_v = a_m N^{1/3}$, where N is the number of monomers in the aggregate and a_m is the monomer's radius of aggregates. We have found from a literature survey that most of the work related to interstellar extinction considered a normal size range of 0.001 to 0.250 μm, with a size distribution (mainly an MRN distribution) (Jones 1988; Whittet 2003; Vaidya et al. 2007; Das et al. 2010). They found an 'optimum' for the range of the cluster size generally used. The above size range of the monomer is more or less capable of evaluating an average observed interstellar extinction curve. If we consider $N = 64$ and a_m in the range 0.001 to 0.065 μm (with a step size of 0.004 μm), then a_v will be 0.004 to 0.26 μm. This size range is almost comparable to the size range used by other investigators.

We use JaSTA-2 (second version of the Java Superposition T-matrix Application) (Halder & Das 2017), which is an upgraded version of JaSTA (Halder et al. 2014), to execute our computations. This routine is based on Mackowski & Mishchenko (1996)'s Superposition T-matrix code. All versions of JaSTA are freely available for download from

Table 1 Coefficients of Eq. (2) are shown for $\lambda = 0.11, 0.20, 0.30$ and 0.90 μm

λ	k	A_k	B_k	C_k
0.11 μm	0.001	−13.245	46.876	−33.026
	0.01	−12.937	45.862	−32.263
	0.1	−10.123	36.537	−25.149
	0.5	−2.651	10.490	−3.731
	1.0	−0.346	1.555	4.661
0.20 μm	0.001	−7.815	36.995	−33.540
	0.01	−7.572	35.969	−32.527
	0.1	−5.439	26.899	−23.511
	0.5	−0.969	6.779	−2.590
	1.0	0.010	1.141	4.359
0.30 μm	0.001	1.651	2.290	−5.271
	0.01	1.647	2.191	−5.054
	0.1	1.589	1.335	−3.095
	0.5	3.527	−0.999	3.939
	1.0	0.681	−0.749	5.243
0.90 μm	0.001	0.217	−0.278	0.032
	0.01	0.217	−0.285	0.068
	0.1	0.213	−0.363	0.429
	0.5	0.230	−0.794	2.046
	1.0	0.328	−1.543	4.092

Table 2 Coefficients of Eq. (2a)–(2c) at $\lambda = 0.11, 0.20, 0.30$ and 0.90 μm

		Coeff-1	Coeff-2	Coeff-3	Coeff-4
$\lambda = 0.11$ μm	A_k	10.161	−31.889	34.662	−13.280
	B_k	−26.328	94.623	−113.730	46.990
	C_k	11.321	−58.956	85.407	−33.111
$\lambda = 0.20$ μm	A_k	15.474	−35.001	27.379	−7.842
	B_k	−60.269	139.790	−115.490	37.110
	C_k	55.593	−131.620	114.040	−33.654
$\lambda = 0.30$ μm	A_k	1.586	−2.127	−0.431	1.652
	B_k	−8.473	16.673	−11.251	2.302
	C_k	10.310	−24.081	24.309	−5.295
$\lambda = 0.90$ μm	A_k	0.001	0.171	−0.060	0.217
	B_k	−0.024	−0.430	−0.812	−0.277
	C_k	0.002	0.053	4.009	0.028

http://ausastro.in/jasta.html. Computations with the T-matrix code are fast and this technique gives rigorous solutions for randomly oriented ensembles of spheres. It can be noted that the results obtained from the DDA approach and the T-matrix approach are almost same. Kimura (2001) showed the results with aggregates using the DDA and the T-matrix code, and found almost the same results with both codes. We perform the computations with a wide range of complex refractive indices (n = 1.4, 1.5, 1.6, 1.7, 1.8, 1.9 and 2.0, and k = 0.001, 0.01, 0.05, 0.1, 0.3, 0.5, 0.7 and 1.0) and wavelengths (0.11, 0.12, 0.13, 0.16, 0.175, 0.185, 0.20, 0.207, 0.22, 0.23, 0.26, 0.30, 0.365, 0.40, 0.55, 0.6, 0.7, 0.8, 0.90 and 3.4 μm). In general, the range of n and k which is considered in our work almost covers the range of complex refractive indices of silicate and carbon at different wavelengths. The numerical computation in the present work has been executed with a BCCA cluster consisting of 64 monomers.

We present the results for $a_m = 0.001, 0.017, 0.041$ and 0.065 μm where a_v is given by 0.004, 0.068, 0.16 and 0.26 μm. The monomer size parameter (x =

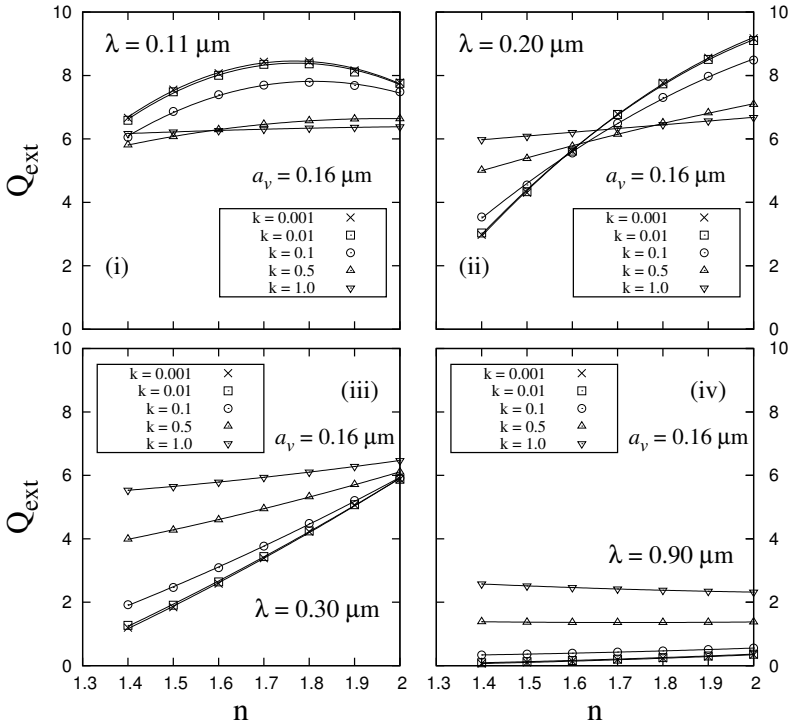

Fig. 1 Extinction efficiency ($Q_{\rm ext}$) is plotted against the real part of the refractive index (n) for k = 0.001, 0.01, 0.1, 0.5 and 1.0 at $a_v = 0.16$ μm. The best fit curves correspond to *quadratic regression* of the form $Q_{\rm ext} = A_k n^2 + B_k n + C_k$ for wavelengths (i) 0.11 μm, (ii) 0.20 μm, (iii) 0.30 μm and (iv) 0.90 μm.

$2\pi a_m/\lambda$) is taken in a range from 0.01 to 1.6. This study mainly concentrates on investigation of correlation among $Q_{\rm ext}$, (n, k), λ and x.

3 RESULTS

3.1 Dependence on Monomer Size (a_m)

3.1.1 Correlation between $Q_{\rm ext}$ and n

We perform the computations with a wide range of complex refractive indices ($1.4 \le n \le 2.0$ and $0.001 \le k \le 1.0$) and wavelengths of incident radiation ($0.11 \le \lambda \le 3.4$ μm). To study the dependence of n and k on the extinction efficiency ($Q_{\rm ext}$), we can either plot $Q_{\rm ext}$ versus k by keeping n fixed or plot $Q_{\rm ext}$ versus n by keeping k fixed. We first show the results for moderate size of the cluster, i.e., at $a_v = 0.16$ μm. The results at the other three sizes are also presented thereafter.

We plot $Q_{\rm ext}$ versus n at $a_v = 0.16$ μm, for k = 0.001, 0.01, 0.1, 0.5 and 1.0 (although we have executed the code with all eight values of k mentioned above), in a single frame, for $\lambda = 0.11, 0.20, 0.30$ and 0.90 μm, which is shown in Figure 1. It can be noted that the plots are shown for four wavelengths although the computations have been performed for all the wavelengths.

It can be observed from Figure 1 that if k is fixed at any value between 0.001 and 1.0, $Q_{\rm ext}$ increases with an increase of n from 1.4 to 2.0 at all wavelengths. However, a small decrease in $Q_{\rm ext}$ is also noticed at $\lambda = 0.11$ μm when $n > 1.7$ and k is low. The variation of $Q_{\rm ext}$ with n is small when $k \ge 0.5$. The value of $Q_{\rm ext}$ is small when λ is large, i.e. $Q_{\rm ext}$ decreases when size parameter of the monomer ($x = 2\pi a_m/\lambda$) decreases. We have also investigated that the variation of $Q_{\rm ext}$ with n is very small when $\lambda \ge 0.70$ μm.

We have found that $Q_{\rm ext}$ and n can be fitted by *quadratic regression* where the *coefficient of determination* [1] (R^2) for each equation is ≈ 0.99. The best fit equation is given by

$$\begin{aligned} &Q_{\rm ext} = A_k n^2 + B_k n + C_k, \\ &1.4 \le n \le 2.0, \quad 0.001 \le k \le 1, \end{aligned} \tag{2}$$

where A_k, B_k and C_k are k-dependent coefficients of Equation (2).

[1] *The coefficient of determination* is a key output of regression analysis which is interpreted as the proportion of the variance in the dependent variable that ranges from 0 to 1. A higher coefficient is an indicator of a better goodness of fit for the observations.

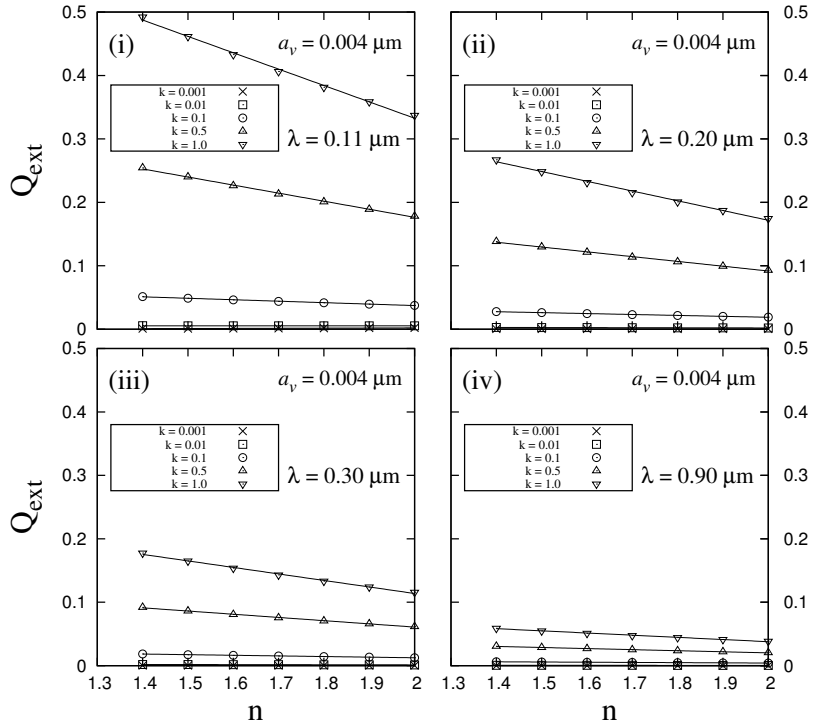

Fig. 2 Extinction efficiency ($Q_{\rm ext}$) is plotted against the real part of the refractive index (n) for k = 0.001, 0.01, 0.1, 0.5 and 1.0 at $a_v = 0.004$ μm. The best fit curves correspond to *linear regression* for wavelengths (i) 0.11 μm, (ii) 0.20 μm, (iii) 0.30 μm and (iv) 0.90 μm.

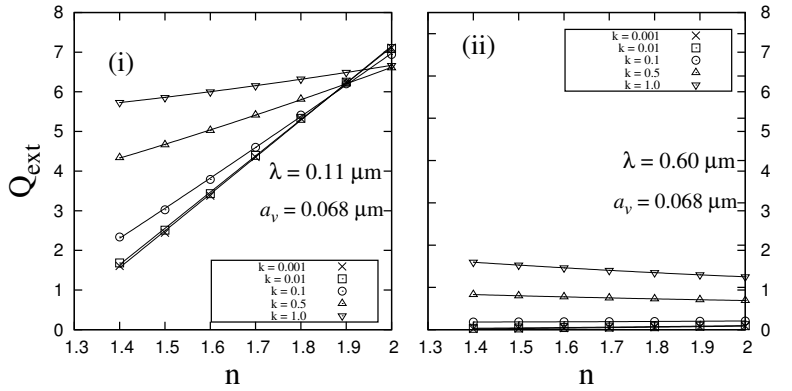

Fig. 3 Extinction efficiency ($Q_{\rm ext}$) is plotted against the real part of the refractive index (n) for k = 0.001, 0.01, 0.1, 0.5 and 1.0 at $a_v = 0.068$ μm. The best fit curves correspond to *quadratic regression* for wavelengths (i) 0.11 μm and (ii) 0.60 μm.

The coefficients obtained for different values of k (only five values of k are shown) are depicted in Table 1. If we plot coefficients A_k, B_k and C_k versus k (where k = 0.001, 0.01, 0.05, 0.1, 0.3, 0.5, 0.7 and 1.0), we find that the best fit curves correspond to *cubic regression*, which have $R^2 \approx 0.99$. We do not show any figures in this case.

The coefficients are correlated with k by the relations:

$$A_k = D_1k^3 + D_2k^2 + D_3k + D_4 \ , \qquad \text{(2a)}$$

$$B_k = E_1k^3 + E_2k^2 + E_3k + E_4 \ , \qquad \text{(2b)}$$

$$C_k = F_1k^3 + F_2k^2 + F_3k + F_4 \ . \qquad \text{(2c)}$$

All coefficients of Equation (2a)–(2c) are shown in Table 2. Thus knowing the coefficients, the extinction ef-

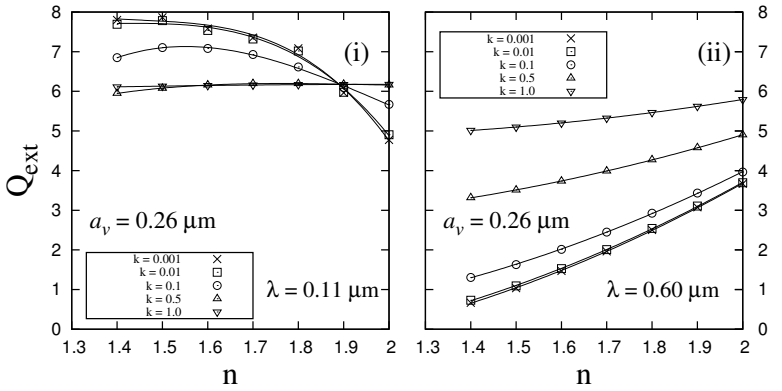

Fig. 4 Extinction efficiency ($Q_{\rm ext}$) is plotted against the real part of the refractive index (n) for k = 0.001, 0.01, 0.1, 0.5 and 1.0 at $a_v = 0.26$ μm. The best fit curves correspond to *cubic regression* at (i) $\lambda = 0.11$ μm and *quadratic regression* at (ii) $\lambda = 0.60$ μm.

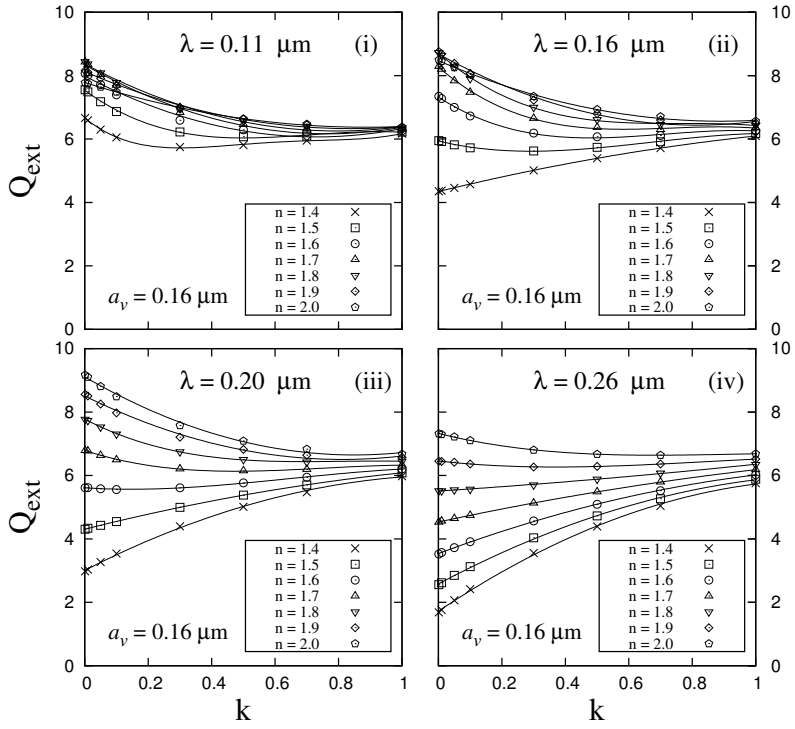

Fig. 5 Extinction efficiency ($Q_{\rm ext}$) is plotted against the imaginary part of the refractive index (k) at λ = 0.11, 0.16, 0.20 and 0.26 μm at $a_v = 0.16$ μm. The best fit curves correspond to polynomial regression equation where the degree of equation depends on the value of n and λ (please see Sect. 3.1.2 for details).

ficiency ($Q_{\rm ext}$) can be calculated for any value of n and k from Equation (2).

In Figure 2, we report the results for $a_v = 0.004$ μm at $\lambda = 0.11, 0.20, 0.30$ and 0.90 μm. A strong *linear* correlation between $Q_{\rm ext}$ and n is seen at this size for all wavelengths from 0.11 to 3.4 μm.

In Figure 3, we plot $Q_{\rm ext}$ versus n for $a_v = 0.068$ μm at $\lambda = 0.11$ μm and 0.60μm. We have found that the nature is *quadratic* at all wavelengths from 0.11 to 3.4 μm. Finally, we show the results for $a_v = 0.26$ μm at $\lambda = 0.11$ μm and 0.60 μm, in Figure 4. We have noticed that $Q_{\rm ext}$ and n are correlated via a *cubic* regression at 0.11 μm, whereas the dependence is *quadratic* at other higher wavelengths. We do not show any equation or table in the above three cases. In summary, we can conclude that the correlation between $Q_{\rm ext}$ and n is *linear*

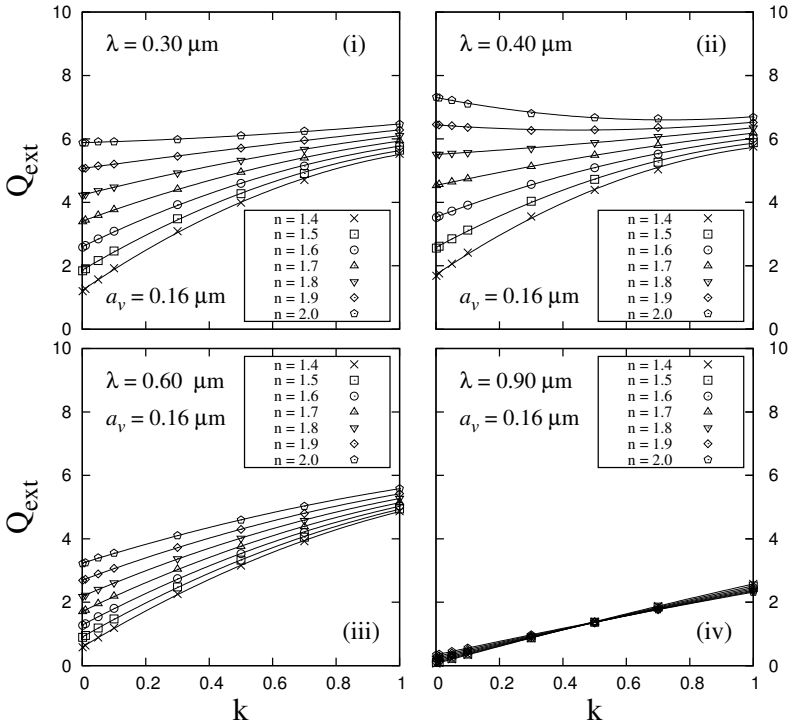

Fig. 6 Extinction efficiency ($Q_{\rm ext}$) is plotted against the imaginary part of the refractive index (k) for n = 1.4, 1.5, 1.6, 1.7, 1.8, 1.9 and 2.0 at $a_v = 0.16$ μm. The best fit curves correspond to *quadratic regression* of the form $Q_{\rm ext} = A'_n k^2 + B'_n k + C'_n$ for wavelengths (i) 0.30 μm, (ii) 0.40 μm, (iii) 0.60 μm and (iv) 0.90 μm.

when the cluster size is small whereas the correlation is *quadratic* at moderate and higher sizes of the cluster.

3.1.2 Correlation between $Q_{\rm ext}$ and k

We now plot $Q_{\rm ext}$ versus k for n = 1.4, 1.5, 1.6, 1.7, 1.8, 1.9 and 2.0, at $a_v = 0.16$ μm where λ is taken between 0.11 μm and 3.4 μm. When λ is between 0.11 μm and 0.26 μm, we have found that $Q_{\rm ext}$ and k can be fitted via a polynomial regression equation where the degree of equation depends on the value of n and λ.

In Figure 5 we show the plots for $\lambda = 0.11, 0.16, 0.20$ and 0.26 μm. At $\lambda = 0.11$ μm, we find that $Q_{\rm ext}$ and k are correlated by (i) *quartic* regression when $n = 1.4$, (ii) *cubic* regression when $n = 1.5$ and (iii) *quadratic* regression when n = 1.6, 1.7, 1.8, 1.9 and 2.0. Further, at $\lambda = 0.16$ μm, the correlation is *cubic* when n = 1.5, 1.6, 1.7 and 1.8 and *quadratic* when n = 1.4, 1.9 and 2.0. The correlation at $\lambda = 0.20$μm is *cubic* when n = 1.6, 1.7 and 1.8 and *quadratic* when n = 1.4, 1.5, 1.9 and 2.0. We also note that the correlation at 0.26 μm is *quadratic* when n = 1.4, 1.5, 1.6, 1.7 and 1.8, and *cubic* when n = 1.9 and 2.0. At low values of n, $Q_{\rm ext}$ increases with an increase of k whereas the trend is exactly opposite when n is high, e.g., at $\lambda = 0.20$ μm, $Q_{\rm ext}$ increases with k when $n \leq 1.6$, but it decreases when $n \geq 1.7$. The vertical range of $Q_{\rm ext}$ in the plot also decreases when k increases. This range is maximum at $k = 0.001$ and minimum at $k = 1.0$.

In Figure 6, we show the plots for $0.30 \leq \lambda \leq 3.4$ μm and we have found that the fit is *quadratic* for all values of n. An increase in $Q_{\rm ext}$ with k is noticed at almost all wavelengths. The vertical range of $Q_{\rm ext}$ also decreases when k increases. Further, the plot of $Q_{\rm ext}$ with k is the same at all values of n when λ is high (please see Fig. 6(iv)).

The best fit equation in the wavelength range 0.30 μm to 3.4 μm is given by

$$Q_{\rm ext} = A_n k^2 + B_n k + C_n \ , \quad 1.4 \leq n \leq 2.0, \ \ 0.001 \leq k \leq 1 \tag{3}$$

where A_n, B_n and C_n are n-dependent coefficients of Equation (3).

The coefficients obtained for different values of k are shown in Table 3. If we plot coefficients A_n, B_n and C_n versus n (figures are not shown), we note that the best fit

curves correspond to *quadratic regression*, which have $R^2 \approx 0.99$.

Thus coefficients are given by

$$A_n = D_1' k^2 + D_2' k + D_3' \ , \tag{3a}$$

$$B_n = E_1' k^2 + E_2' k + E_3' \ , \tag{3b}$$

$$C_n = F_1' k^2 + F_2' k + F_3' \ . \tag{3c}$$

All coefficients of Equation (3a)–(3c) are shown in Table 4. Thus, knowing the coefficients of Equation (3a-3c), the extinction efficiency ($Q_{\rm ext}$) can also be estimated for any value of n and k from Equation (3).

In Figure 7, we plot $Q_{\rm ext}$ against k for $a_v = 0.004\,\mu$m at $\lambda = 0.11, 0.30, 0.60$ and $0.90\,\mu$m, although the computations have been performed for a wide range of wavelengths from 0.11 to 3.4 μm. We observe a *linear* dependence at this size for all wavelengths. This linear nature becomes *quadratic* when the size of the cluster is $a_v = 0.068\,\mu$m.

Figure 8 shows the results for $a_v = 0.068\,\mu$m at λ = 0.11 μm and 0.60 μm. In Figure 9, the results obtained for $a_v = 0.26\,\mu$m are plotted. In this case, the nature of the dependence looks similar to $a_v = 0.16\,\mu$m. $Q_{\rm ext}$ and k are correlated via polynomial regression equation (of degree 2, 3 or 4) where the degree of the equation depends on the real part of the refractive index (n) at ($\lambda = 0.11\,\mu$m) (please see the caption of Fig. 9). The nature is quadratic when $\lambda > 0.11\,\mu$m. In summary, we can conclude that the relationship of $Q_{\rm ext}$ on k depends on the cluster size. The correlation is linear for small size and quadratic/cubic for moderate and higher sizes.

It is important to mention that the real part of the complex index of refraction (n) controls the effective phase speed of electromagnetic waves propagating through the medium, while the imaginary part k describes the rate of absorption of the wave. In any material, n and k are not free to vary independently of one another but rather are tightly coupled to one another via the so-called Kramer-Kronig relations. Therefore, the results presented above are quite expectable.

3.2 Dependence on Wavelength of Radiation (λ)

We now study the dependence of $Q_{\rm ext}$ on λ for a particular set of (n, k) in the case of $a_v = 0.16\,\mu$m only. We observe the following results:

(i) For n = 1.4, 1.5 and 1.6, $Q_{\rm ext}$ versus λ can be fitted via a *quartic* regression for k = 0.001, 0.01, 0.05, 0.1, 0.3, 0.5, 0.7 and 1.0 (please see Fig. 10).

(ii) For n = 1.7, 1.8, 1.9 and 2.0, $Q_{\rm ext}$ versus λ can be fitted via a *quartic* regression in the wavelength range $0.11 - 0.40\,\mu$m [Fig. 11(i,iv) and Fig. 12(i,iv)] and a *quadratic* regression in the wavelength range $0.55 - 0.90\,\mu$m [Fig. 11(ii,v) and Fig. 12(ii,v)] for k = 0.001, 0.01, 0.05, 0.1 and 0.3. Further, $Q_{\rm ext}$ versus λ can be fitted via a *quartic* regression in the wavelength range $0.11 - 0.90\,\mu$m for higher values of k = 0.5, 0.7 and 1 [Fig. 11(iii,vi) and Fig. 12(iii,vi)]. We did not include the plots for $\lambda = 3.4\,\mu$m.

It can be noticed from Figures 10, 11 and 12 that $Q_{\rm ext}$ decreases with increase of λ when $n \leq 1.6$. When $n \geq 1.7$, $Q_{\rm ext}$ initially increases with increase of λ and reaches a maximum value, then it starts decreasing if λ is increased further. We also observe that $Q_{\rm ext}$ is maximum at k = 0.001 and minimum at k = 1.0 when $\lambda = 0.11\,\mu$m, but this trend changes at a critical value of wavelength (λ_c) where an exactly opposite nature is noticed. We see that λ_c is (i) 0.16 μm at $n = 1.4$, (ii) 0.185 μm at $n = 1.5$, (iii) 0.207 μm at $n = 1.6$, (iv) 0.22 μm at $n = 1.7$, (v) 0.26 μm at $n = 1.8$, (vi) 0.26 μm at $n = 1.9$ and (vii) 0.30 μm at $n = 1.4$. The value of $Q_{\rm ext}$ is maximum at k = 1.0 when $\lambda > \lambda_c$. We do not show any equations or tables in this case.

3.3 Dependence on the Size Parameter of Monomer (x)

We now study the dependence of $Q_{\rm ext}$ on the size parameter of monomer ($x = 2\pi a_m/\lambda$) for n = 1.4, 1.5, 1.6, 1.7, 1.8, 1.9 and 2.0, and k = 0.001, 0.01, 0.05, 0.1, 0.3, 0.5, 0.7 and 1.0. A wide range of size parameter, $0.01 \leq x \leq 1.6$ (where $N = 64$), is considered to investigate the correlation between $Q_{\rm ext}$ and x. The results are plotted in Figures 13, 14, 15 and 16 for $k = 0.001, 0.01, 0.1$ and 1.0, respectively. It can be seen from the figures that if x is fixed at any value between 0.01 and 1.6, $Q_{\rm ext}$ increases with an increase of n. This increase is prominent when $x > 0.2$. The vertical range of $Q_{\rm ext}$ also increases with an increase of n from 1.4 to 2.0. This range is maximum (i) at $x = 1.4$ in the case of $k = 0.001$ (where $Q_{\rm ext}$ = [9.34, 3.45]), (ii) at $x = 1.4$ in the case of $k = 0.01$ (where $Q_{\rm ext}$ = [9.26, 3.50]), (iii) at $x = 1.4$ in the case of $k = 0.1$ (where $Q_{\rm ext}$ = [8.56, 3.90]), and (iv) at $x = 1.12$ in the case of $k = 1.0$ (where $Q_{\rm ext}$(max) = [6.74, 5.88]). The slope of the $Q_{\rm ext}$ versus x curve increases with the increase of n from 1.4 to 2.0, which can be noted for all values of k. It is also interest-

Table 3 Coefficients of Equation (3) at $\lambda = 0.30, 0.40, 0.60$ and 0.90 μm

λ	n	A_n	B_n	C_n
0.30 μm	1.4	–2.579	6.890	1.195
	1.5	–2.107	5.844	1.896
	1.6	–1.630	4.774	2.632
	1.7	–1.148	3.678	3.401
	1.8	–0.661	2.556	4.204
	1.9	–0.169	1.410	5.041
	2.0	0.327	0.238	5.911
0.40 μm	1.4	–1.769	6.047	0.579
	1.5	–1.655	5.675	0.912
	1.6	–1.519	5.256	1.290
	1.7	–1.362	4.789	1.712
	1.8	–1.184	4.274	2.178
	1.9	–0.984	3.712	2.688
	2.0	–0.763	3.102	3.242
0.60 μm	1.4	–0.727	4.222	0.198
	1.5	–0.704	4.081	0.307
	1.6	–0.676	3.931	0.433
	1.7	–0.642	3.771	0.574
	1.8	–0.602	3.602	0.731
	1.9	–0.556	3.423	0.905
	2.0	–0.505	3.234	1.094
0.90 μm	1.4	–0.260	2.771	0.064
	1.5	–0.257	2.674	0.100
	1.6	–0.250	2.575	0.139
	1.7	–0.240	2.475	0.183
	1.8	–0.227	2.374	0.231
	1.9	–0.210	2.272	0.284
	2.0	–0.190	2.169	0.341

Table 4 Coefficients of Equation (3a–3c) at $\lambda = 0.30, 0.40, 0.60$ and 0.90 μm

λ		Coeff-1	Coeff-2	Coeff-3
0.30 μm	A_n	0.243	4.016	–8.679
	B_n	–1.269	–6.771	18.857
	C_n	1.682	2.142	–5.101
0.40 μm	A_n	1.069	–1.956	–1.126
	B_n	–2.385	3.201	6.241
	C_n	2.202	–3.048	0.530
0.60 μm	A_n	0.290	–0.614	–0.434
	B_n	–0.481	–0.010	5.179
	C_n	0.796	–1.214	0.337
0.90 μm	A_n	0.171	–0.466	0.056
	B_n	–0.060	–0.799	4.008
	C_n	0.217	–0.278	0.028

ing to notice that the vertical range of $Q_{\rm ext}$ at $x = 1.6$ decreases with the increase of k and is lowest at $k = 1.0$. Further, the $Q_{\rm ext}$ value does not depend much on n for highly absorptive particles ($k = 1.0$) when $x < 0.5$. The variation is also small when $x > 0.5$.

We have found that $Q_{\rm ext}$ and x can be fitted by a *cubic regression* for all values of n except 2.0, in case of $k = 0.001, 0.01$ and 0.1. The coefficient of determination (R^2) for each equation is ≈ 0.99. The best fit equation is

Table 5 All Coefficients of Eqs. (4), (5) and (6)

k	n	α_1	α_2	α_3	α_4		
0.001	1.4	–0.425	2.844	–0.728	0.034		
	1.5	–1.179	5.041	–1.316	0.056		
	1.6	–2.239	7.681	–1.976	0.082		
	1.7	–3.654	10.775	–2.712	0.109		
	1.8	–5.362	14.173	–3.475	0.136		
	1.9	–7.242	17.624	–4.175	0.158		
0.01	1.4	–0.502	2.931	–0.660	0.032		
	1.5	–1.248	5.085	–1.231	0.055		
	1.6	–2.312	7.713	–1.888	0.080		
	1.7	–3.714	10.772	–2.617	0.107		
	1.8	–5.367	14.060	–3.346	0.133		
	1.9	–7.189	17.404	–4.011	0.153		
0.1	1.4	–0.891	3.035	0.273	0.023		
	1.5	–1.588	4.882	–0.186	0.038		
	1.6	–2.540	7.120	–0.715	0.055		
	1.7	–3.726	9.652	–1.276	0.072		
	1.8	–5.100	12.358	–1.829	0.087		
	1.9	–6.569	15.046	–2.302	0.097		
k	n	β_1	β_2	β_3	β_4	β_5	
0.001	2.0	–2.164	–2.689	15.031	–3.120	0.102	
0.01	2.0	–1.926	–3.285	15.343	–3.097	0.103	
0.1	2.0	0.323	–8.985	18.392	–2.869	0.109	
k	n	γ_1	γ_2	γ_3	γ_4	γ_5	γ_6
1.0	1.4	–2.709	12.371	–18.540	6.182	8.466	–0.009
	1.5	–2.973	14.016	–22.167	9.438	7.576	–0.003
	1.6	–3.253	15.774	–26.024	12.846	6.686	0.005
	1.7	–3.540	17.603	–30.058	16.378	5.800	0.014
	1.8	–3.861	19.625	–34.440	20.118	4.901	0.024
	1.9	–4.222	21.861	–39.192	24.073	3.988	0.035
	2.0	–4.625	24.319	–44.317	28.233	3.061	0.047

given by

$$Q_{\rm ext} = \alpha_1 x^3 + \alpha_2 x^2 + \alpha_3 x + \alpha_4, \qquad (4)$$

where α_1, α_2, α_3 and α_4 are n-dependent coefficients of Equation (4). The coefficients are presented in Table 5.

However, the best fit equation in case of $n = 2.0$ corresponds to a *quartic regression* for $k = 0.001, 0.01$ and 0.1, which is given by

$$Q_{\rm ext} = \beta_1 x^4 + \beta_2 x^3 + \beta_3 x^2 + \beta_4 x + \beta_5, \qquad (5)$$

where β_1, β_2, β_3, β_4 and β_5 are n-dependent coefficients, shown in Table 5.

The correlation between $Q_{\rm ext}$ and x is found to be a *quintic regression* for all values of n at $k = 1.0$. The best fit equation is given by

$$Q_{\rm ext} = \gamma_1 x^5 + \gamma_2 x^4 + \gamma_3 x^3 + \gamma_4 x^2 + \gamma_5 x + \gamma_6, \quad (6)$$

where $\gamma_1, \gamma_2, \gamma_3, \gamma_4, \gamma_5$ and γ_6 are n-dependent constants of Equation (6). The constants are given in Table 5.

Equations (4), (5) and (6) are very useful in estimating $Q_{\rm ext}$, where one can generate a large data set for $Q_{\rm ext}$ for a selected set of n, k, a_m and λ.

4 RESULTS FROM CORRELATION EQUATIONS

In the previous sections, we have obtained a set of correlation equations which can be used to calculate the extinction efficiency of dust aggregates with a wide range of size of aggregates and wavelength of radiation. We first calculate $Q_{\rm ext}$ from relations (2) and (3) for BCCA particles with $N = 64$ and $a_m = 0.041\,\mu$m, for selected values of n, k and λ. The calculated values are compared with the computed values obtained using the Superposition T-matrix code. The results are shown in Tables 6 and 7. We also estimate $Q_{\rm ext}$ using relations

Table 6 $Q_{\rm ext}$ for selected values of n and k from the relation (using Eq. (2)) and computations (from the simulations) where $a_m = 0.041$ μm and $0.11 \leq \lambda \leq 3.4$ μm. The difference between correlation equation and computed value is Diff. = $|Q_{\rm ext}$ (corr) $- Q_{\rm ext}$ (comp)|.

λ	n	k	$Q_{\rm ext}$ (corr)	$Q_{\rm ext}$ (comp)	Diff.
0.11	1.5	0.001	7.487	7.555	0.068
	1.7	0.01	8.316	8.353	0.037
	1.9	0.1	7.729	7.683	0.046
0.20	1.5	0.001	4.368	4.305	0.063
	1.7	0.01	6.738	6.771	0.033
	1.9	0.1	7.963	7.975	0.012
0.30	1.5	0.001	1.881	1.842	0.039
	1.7	0.01	3.431	3.441	0.010
	1.9	0.1	5.179	5.205	0.026
0.40	1.5	0.001	0.906	0.895	0.011
	1.7	0.01	1.753	1.749	0.004
	1.9	0.1	3.057	3.070	0.013
0.55	1.5	0.001	0.390	0.388	0.002
	1.7	0.01	0.768	0.768	0.000
	1.9	0.1	1.513	1.513	0.000
0.70	1.5	0.001	0.205	0.203	0.002
	1.7	0.01	0.406	0.406	0.000
	1.9	0.1	0.879	0.880	0.001
0.90	1.5	0.001	0.103	0.102	0.001
	1.7	0.01	0.208	0.208	0.000
	1.9	0.1	0.508	0.509	0.001
3.4	1.5	0.001	0.002	0.002	0.001
	1.7	0.01	0.008	0.009	0.001
	1.9	0.1	0.056	0.056	0.001

Table 7 $Q_{\rm ext}$ for selected values of n and k from the relation (using Eq. (3)) and computations (from the simulations) where $a_m = 0.041\,\mu$m and $0.30 \leq \lambda \leq 3.4\,\mu$m . The difference between correlation equation and computed value is Diff. = $|Q_{\rm ext}$ (corr) $- Q_{\rm ext}$ (comp)|.

λ	n	k	$Q_{\rm ext}$ (corr)	$Q_{\rm ext}$ (comp)	Diff.
0.30	1.5	0.001	1.902	1.842	0.060
	1.7	0.01	3.438	3.441	0.003
	1.9	0.1	5.180	5.205	0.025
0.40	1.5	0.001	0.918	0.895	0.023
	1.7	0.01	1.760	1.749	0.011
	1.9	0.1	3.049	3.070	0.021
0.55	1.5	0.001	0.394	0.388	0.006
	1.7	0.01	0.770	0.768	0.002
	1.9	0.1	1.513	1.513	0.000
0.70	1.5	0.001	0.205	0.203	0.002
	1.7	0.01	0.407	0.406	0.001
	1.9	0.1	0.879	0.880	0.001
0.90	1.5	0.001	0.102	0.102	0.000
	1.7	0.01	0.208	0.208	0.000
	1.9	0.1	0.509	0.509	0.000
3.4	1.5	0.001	0.002	0.002	0.000
	1.7	0.01	0.008	0.009	0.001
	1.9	0.1	0.056	0.056	0.000

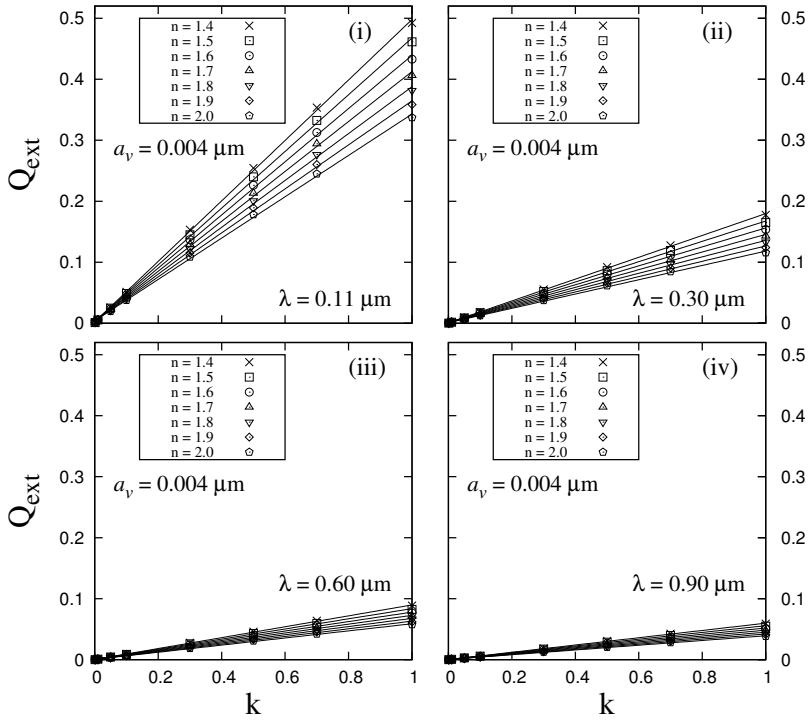

Fig. 7 Extinction efficiency ($Q_{\rm ext}$) is plotted against the imaginary part of the refractive index (k) for n = 1.4, 1.5, 1.6, 1.7, 1.8, 1.9 and 2.0 at $a_v = 0.004$ μm. The best fit curves correspond to *linear regression* for wavelengths (i) 0.11 μm, (ii) 0.30 μm, (iii) 0.60 μm and (iv) 0.90 μm.

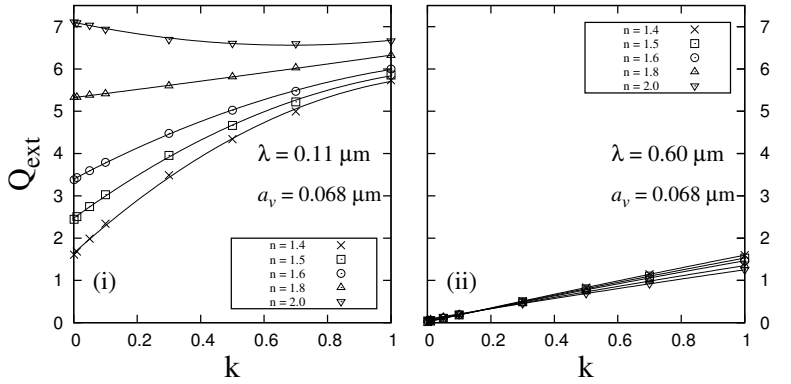

Fig. 8 Extinction efficiency ($Q_{\rm ext}$) is plotted against the imaginary part of the refractive index (k) for n = 1.4, 1.5, 1.6, 1.8 and 2.0 at $a_v = 0.068$ μm. The best fit curves correspond to *quadratic regression* for wavelengths (i) 0.11 μm and (ii) 0.60 μm.

(4), (5) and (6) for selected values of x, n and k, and the result is shown in Table 8. It can be seen that the values obtained from computation match well with the results obtained from correlation equations.

In general, to model the interstellar extinction, one needs to execute the light scattering code with different values of a_m (or a_v) and wavelength (λ), which is very time consuming. Using a size distribution for aggregates, it is possible to obtain the average extinction curves for silicate and graphite (and/or amorphous carbon) particles. With a suitable mixing among them, the extinction curve versus different wavelengths can be generated, which can be fitted well with an observed extinction curve. Some good pieces of work on modeling were already done for aggregate particles. Some preliminary results on modeling interstellar extinction us-

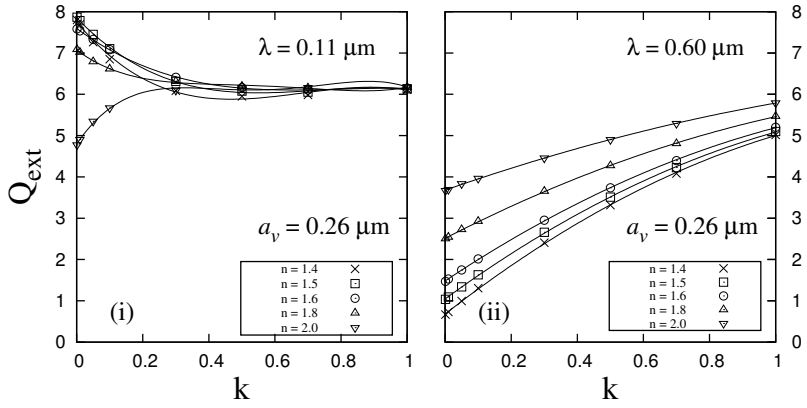

Fig. 9 Extinction efficiency ($Q_{\rm ext}$) is plotted against the imaginary part of the refractive index (k) for n = 1.4, 1.5, 1.6, 1.8 and 2.0 at $a_v = 0.26$ μm. $Q_{\rm ext}$ and k are correlated via polynomial regression equations, where the degree of regression is found to be wavelength dependent: (i) at $\lambda = 0.11$ μm, the correlation is *cubic* for $n = 1.4, 1.5, 1.6, 1.7$ and 2.0, and *quartic* at $n = 1.8$ and 1.9, and (ii) at $\lambda = 0.60$ μm, the correlation is *quadratic* at all values of n.

Table 8 $Q_{\rm ext}$ for selected values of n, k and x from the relation (using Eqs. (4), (5) and (6)) and computations (from the simulations). The difference between correlation equation and computed value is Diff. = $|Q_{\rm ext}$ (corr) $- Q_{\rm ext}$ (comp)|.

x	n	k	$Q_{\rm ext}$ (corr)	$Q_{\rm ext}$ (comp)	Diff.
0.286	1.5	0.001	0.064	0.092	0.028
0.286	1.7	0.01	0.152	0.207	0.055
0.286	1.9	0.1	0.514	0.506	0.008
0.468	1.5	0.001	0.424	0.388	0.036
0.468	1.7	0.01	0.862	0.768	0.094
0.468	2.0	1.0	4.183	4.205	0.022
0.706	1.5	0.001	1.225	1.136	0.089
0.706	1.9	0.1	3.660	3.688	0.028
0.706	2.0	0.1	4.169	4.252	0.083
0.972	1.5	0.001	2.459	2.446	0.013
0.972	1.7	0.01	4.333	4.397	0.064
0.972	2.0	1.0	6.693	6.664	0.029
1.171	1.5	0.001	3.534	3.622	0.088
1.171	1.9	0.1	7.485	7.522	0.037
1.171	2.0	1.0	6.728	6.733	0.005
1.289	1.5	0.001	4.208	4.305	0.097
1.289	1.7	0.01	6.674	6.771	0.097
1.289	1.9	0.1	8.058	7.975	0.083
1.473	1.5	0.001	5.287	5.268	0.019
1.473	1.7	0.01	7.754	7.702	0.052
1.473	1.9	0.1	8.357	8.264	0.093

ing an aggregate dust model were already reported by Bhattacharjee et al. (2010). The present study shows that it is possible to study the extinction properties of interstellar dust aggregates for a given size of the particles and wavelength using relations (4), (5) and (6). The set of correlation equations can be used to estimate the general extinction A_λ using Equation (1) for a given size distribution which will help to model the interstellar extinction curve. At this stage, we are not interested in modeling as this study is primarily intended to investigate the depen-

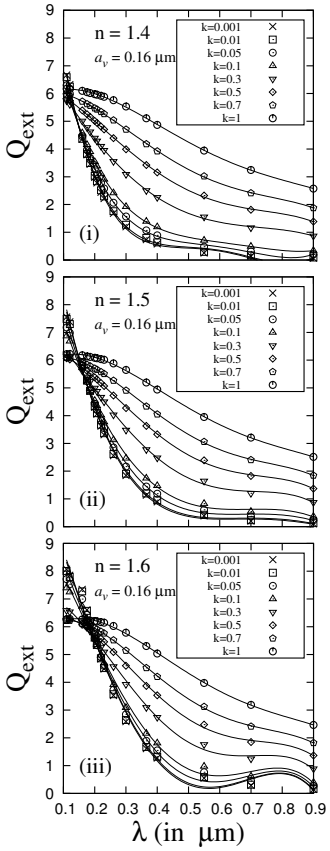

Fig. 10 Extinction efficiency ($Q_{\rm ext}$) is plotted against wavelength (λ) for k = 0.001, 0.01, 0.05, 0.1, 0.3, 0.5, 0.7 and 1.0 at $a_v = 0.16$ μm when (i) $n = 1.4$, (ii) $n = 1.5$ and (iii) $n = 1.6$. The best fit curves correspond to *quartic regression*.

dency of extinction efficiency on size, wavelength and composition of particles. We show how this dependency can be framed with some correlation equations to study the extinction properties of interstellar dust.

Tamanai et al. (2006) experimentally investigated morphological effects on the extinction band in the IR region for amorphous silica (SiO_2) agglomerates. They also compared the measured band profiles with calculations for five cluster shapes applying Mie, T-matrix and DDA codes. Our correlations will also be helpful to study the experimental data, but it is also important to check the input parameters (size parameter, composition, etc.) of the experimental setup before using the correlation equations, because the relations are based on some selected set of parameters.

5 SUMMARY

– We have first studied the dependency of $Q_{\rm ext}$ on size of the aggregates (a_m) to investigate the correlations between $Q_{\rm ext}$ and complex refractive indices (n, k) at a particular size. Computations are performed at four different sizes ($a_v = 0.004, 0.068, 0.16$ and 0.26 μm).

If k is fixed at any value between 0.001 and 1.0, $Q_{\rm ext}$ increases with increase of n from 1.4 to 2.0. $Q_{\rm ext}$ and n are correlated via *linear* regression when the cluster size is small whereas the correlation is *quadratic* at moderate and higher sizes of the cluster. This feature is observed at all wavelengths (UV to optical to IR). We have also found that the variation of $Q_{\rm ext}$ with n is very small when λ is high.

We have observed that $Q_{\rm ext}$ and k are correlated via polynomial regression equation (of degree 2, 3 or 4) where the degree of equation depends on the cluster size, real part of the refractive index of the particles (n) and wavelength (λ) of incident radiation. At $a_v = 0.16$ μm, $Q_{\rm ext}$ and k are found to be correlated with a polynomial regression equation (of degree 2 or 3) when λ is between 0.11 μm and 0.26 μm. However, when $\lambda > 0.26$ μm, we have found that the correlation between them is *quadratic* for all values

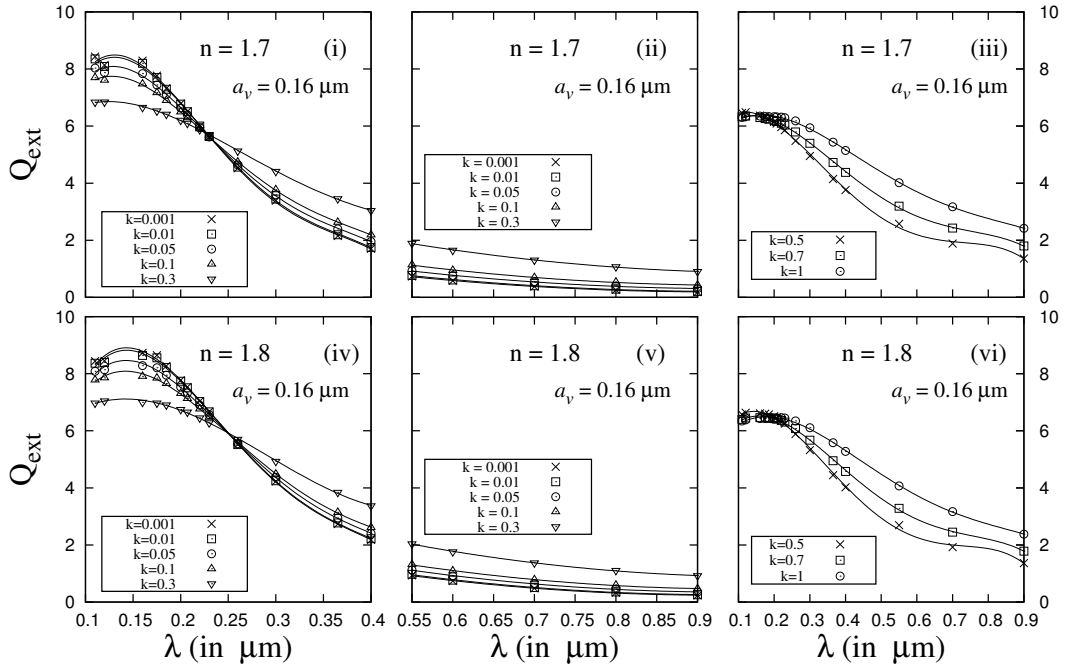

Fig. 11 Extinction efficiency ($Q_{\rm ext}$) is plotted against wavelength of incident radiation (λ) at $a_v = 0.16\,\mu$m. The *left panel* (*top* and *bottom*) shows the plot for the imaginary part of refractive indices (k) = 0.001, 0.01, 0.05, 0.1 and 0.3 in the wavelength range 0.11 μm to 0.40 μm, the *middle panel* (*top* and *bottom*) is for k = 0.001, 0.01, 0.05, 0.1 and 0.3 in the wavelength range 0.55 to 0.90 μm and the *right panel* (*top* and *bottom*) is for k = 0.5, 0.7 and 1 in the wavelength range 0.11 to 0.90 μm. The best fit corresponds to *quartic* regression (*left panel*), *quadratic* regression (*middle panel*) and *quartic* regression (*right panel*). The real part of the refractive index (n) is fixed at 1.7 and 1.8.

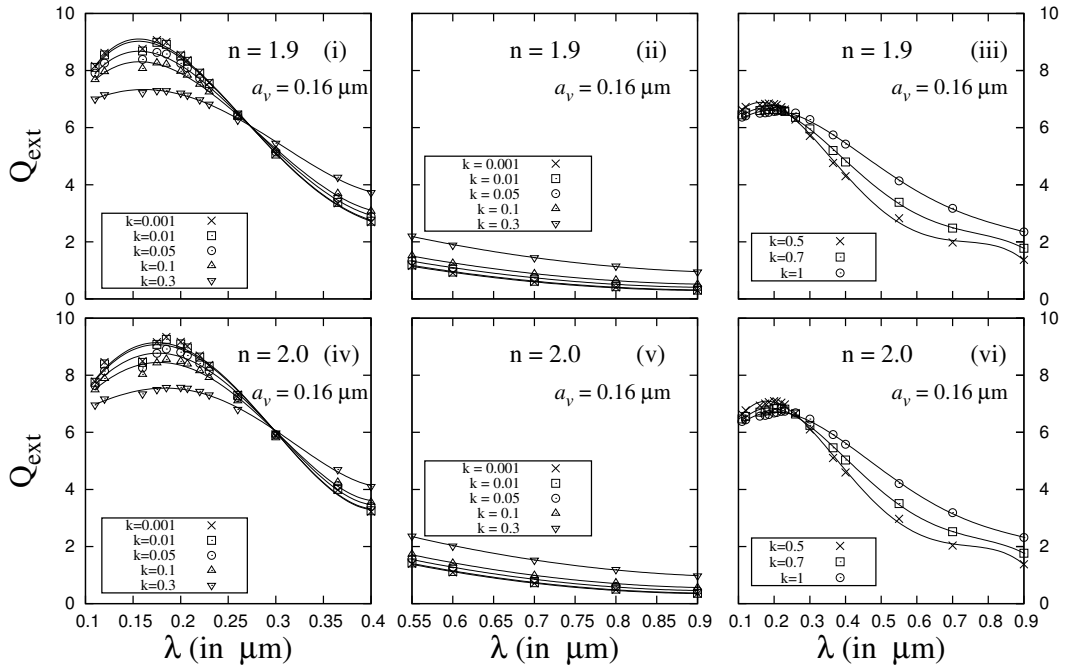

Fig. 12 Same as Fig. 11 but with n = 1.9 and 2.0.

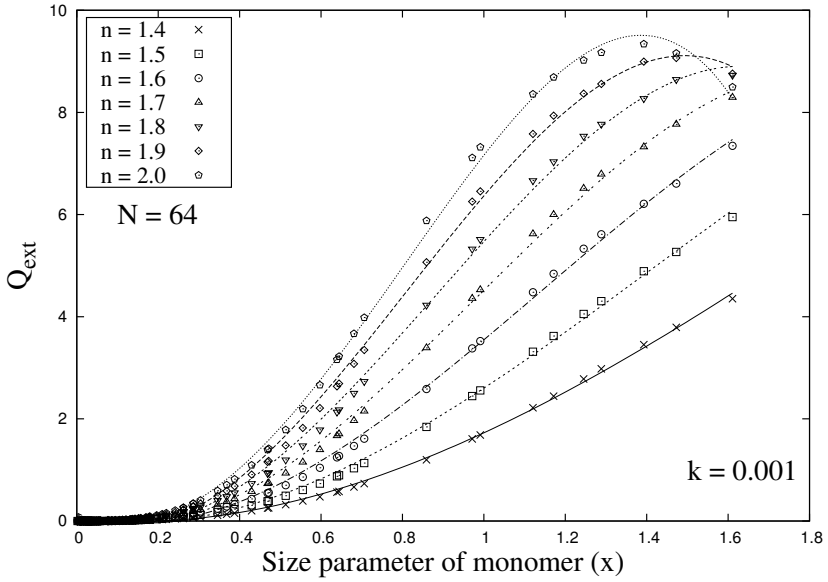

Fig. 13 Extinction efficiency ($Q_{\rm ext}$) is plotted against the size parameter of monomer ($x = 2\pi a_m/\lambda$, where $0.01 \leq x \leq 1.6$) for $N = 64$ and $k = 0.001$. The best fit curves represent a *cubic regression* for all values of n except 2.0, where a *quartic regression* (degree 4) can be noticed. In all cases, the *coefficient of determination* (R^2) ≈ 0.99.

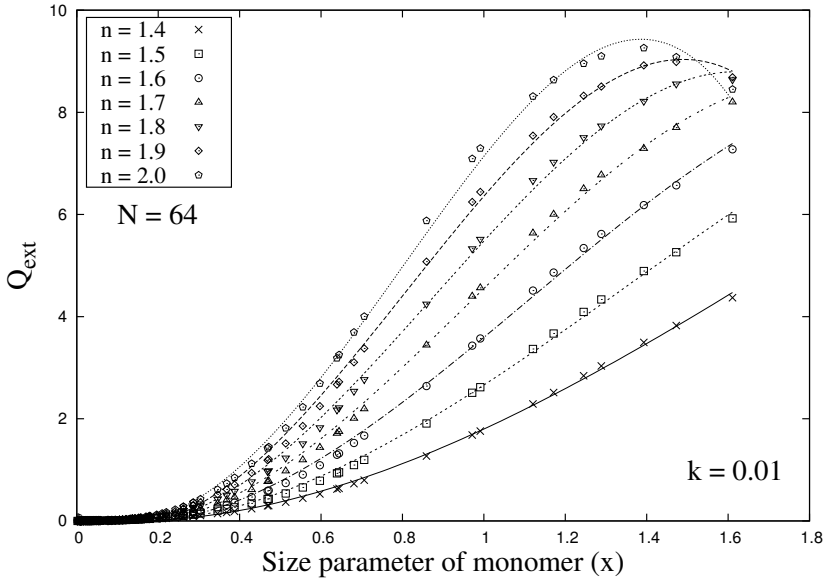

Fig. 14 Same as Fig. 13 but with $k = 0.01$.

of n. The vertical range of $Q_{\rm ext}$ in the plot also decreases when k increases. This range is maximum at $k = 0.001$ and minimum at $k = 1.0$. If we include results for four different cluster sizes, we can summarize that the correlation of $Q_{\rm ext}$ and k depends mainly on cluster size. The correlation is linear for small size and quadratic/cubic/quartic for moderate and higher sizes.

– We study the dependence of $Q_{\rm ext}$ on λ for $a_v = 0.16\,\mu$m. $Q_{\rm ext}$ decreases with increase of λ when $n \leq 1.6$. When $n \geq 1.7$, $Q_{\rm ext}$ initially increases with increase of λ and reaches a maximum value, then it starts decreasing if λ is increased further.

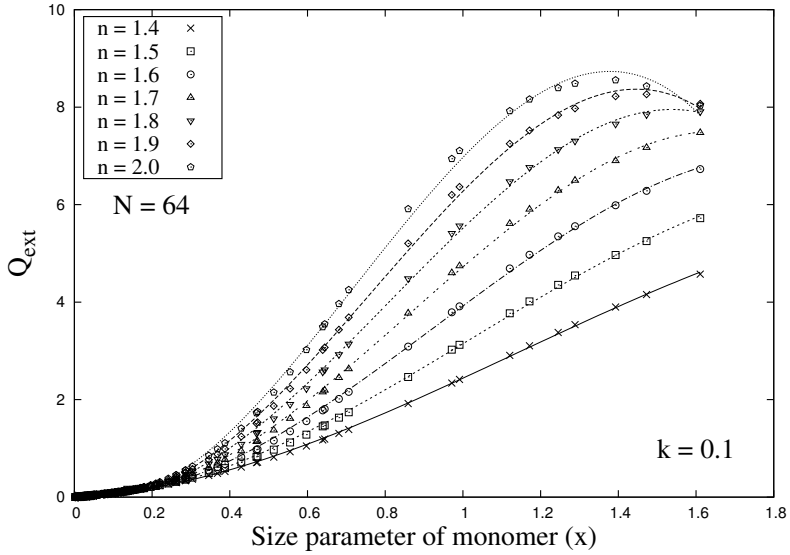

Fig. 15 Same as Fig. 13 but with $k = 0.1$.

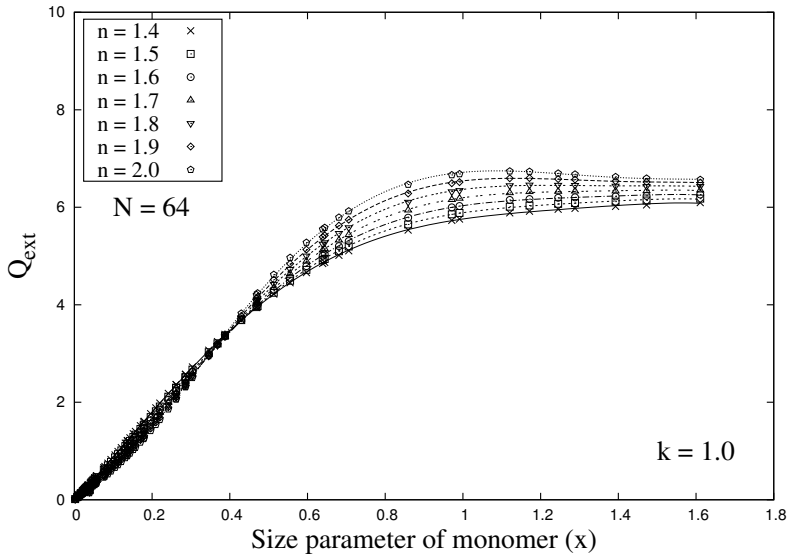

Fig. 16 $Q_{\rm ext}$ is plotted against x for $N = 64$ and $k = 1.0$. In this case, the best fit curves correspond to a *quintic regression* (degree 5) for all values of n. Here, $R^2 \approx 0.99$.

For n = 1.4, 1.5 and 1.6, $Q_{\rm ext}$ versus λ can be fitted via a *quartic* regression for all values of k. For other values of n, the correlation is polynomial regression where the degree of the equation depends on the value of n, k and λ.

– We have found that $Q_{\rm ext}$ and x are correlated via a polynomial regression (of degree 3, 4 or 5) for all values of n. The degree of regression is found to be n and k-dependent.

– The correlation equations can be used to model interstellar extinction for dust aggregates in a wide range of sizes of the aggregates, wavelengths and complex refractive indices.

Acknowledgements We acknowledge Daniel Mackowski and Michael Mishchenko, who made their Multisphere T-matrix (MSTM) code publicly available. We also acknowledge Prithish Halder for help on the execution of JaSTA-2 software package. The reviewer of this

paper is highly acknowledged for useful comments and suggestions.

References

Bhattacharjee, C., Das, H., & Sen, A. 2010, Assam University Journal of Science and Technology, 6, 39

Brownlee, D. E. 1985, Annual Review of Earth and Planetary Sciences, 13, 147

Das, H. S., Das, S. R., Paul, T., Suklabaidya, A., & Sen, A. K. 2008, MNRAS, 389, 787

Das, H. K., Voshchinnikov, N. V., & Il'in, V. B. 2010, MNRAS, 404, 265

Greenberg, J. M., & Hage, J. I. 1990, ApJ, 361, 260

Halder, P., & Das, H. S. 2017, Comp. Phy. Comm. doi:10.1016/j.cpc.2017.08.020

Halder, P., Chakraborty, A., Deb Roy, P., & Das, H. S. 2014, Computer Physics Communications, 185, 2369

Iatì, M. A., Giusto, A., Saija, R., et al. 2004, ApJ, 615, 286

Jones, A. P. 1988, MNRAS, 234, 209

Kimura, H. 2001, J. Quant. Spec. Radiat. Transf., 70, 581

Krueger, F. R., & Kissel, J. 1989, Origins of Life and Evolution of the Biosphere, 19, 87

Mackowski, D. W., & Mishchenko, M. I. 1996, J. Quant. Spectrosc. Radiat. Transfer, 13, 2266

Mathis, J. S., & Whiffen, G. 1989, ApJ, 341, 808

Mazarbhuiya, A. M., & Das, H. S. 2017, Ap&SS, 362, #161

Meakin, P. 1983, Journal of Colloid and Interface Science, 96, 415

Meakin, P. 1984, Phys. Rev. A, 29, 997

Mukai, T., Ishimoto, H., Kozasa, T., Blum, J., & Greenberg, J. M. 1992, A&A, 262, 315

Spitzer, L. 1978, Physical Processes in the Interstellar Medium, 333 (New York: Wiley-Interscience)

Tamanai, A., Mutschke, H., Blum, J., & Neuhäuser, R. 2006, J. Quant. Spec. Radiat. Transf., 100, 373

Vaidya, D. B., & Gupta, R. 1999, A&A, 348, 594

Vaidya, D. B., Gupta, R., & Snow, T. P. 2007, MNRAS, 379, 791

Vaidya, D. B., & Gupta, R. 2009, J. Quant. Spac. Radiat. Transf., 110, 1726

Voshchinnikov, N. V., Il'in, V. B., Henning, T., & Dubkova, D. N. 2006, A&A, 445, 167

Whittet, D. C. B., ed. 2003, in Dust in the Galactic Enviornment, 76 (2nd edn., Bristol: IOP Publishing Ltd.)

Wolff, M. J., Clayton, G. C., Martin, P. G., & Schulte-Ladbeck, R. E. 1994, ApJ, 423, 412

Wolff, M. J., Clayton, G. C., & Gibson, S. J. 1998, ApJ, 503, 815

Wurm, G., & Blum, J. 1998, Icarus, 132, 125